Supporting Information for:

Interaction of Chromium(III) with an *N,N'*-disubstituted Hydroxylamine-(diamido) Ligand. A Combined Experimental and Theoretical Study

Petros A.Tziouris,[†] ConstantinosG.Tsiafoulis,[#] ManolisVlasiou,[‡] Haralampos N. Miras,[*,§] Michael P. Sigalas,[*,⊥] Anastasios D. Keramidas,[*,‡] and Themistoklis A. Kabanos[*,†]

[†]Section of Inorganic and Analytical Chemistry, Department of Chemistry, University of Ioannina, Ioannina 45110, Greece.

[#]NMR Center, University of Ioannina, Ioannina, GR-45110, Greece.

[‡]Department of Chemistry, University of Cyprus, Nicosia 1678, Cyprus.

[§]WestCHEM, School of Chemistry, the University of Glasgow, Glasgow, G12 8QQ, UK.

[⊥]Laboratory of Applied Quantum Chemistry, Department of Chemistry, Aristotle University of Thessaloniki, Thessaloniki 54124, Greece.

*Corresponding authors: Haralampos N. Miras (H. N. M.) E-mail: harism@chem.gla.ac.uk;

Michael P. Sigalas (M. P. S) E-mail: sigalas@chem.auth.gr; Anastasios D. Keramidas (A. D. K.) E-mail: akeramid@ucy.ac.cy; Themistoklis A. Kabanos (T. A. K.) E-mail: tkampano@cc.uoi.gr;

Table of Contents
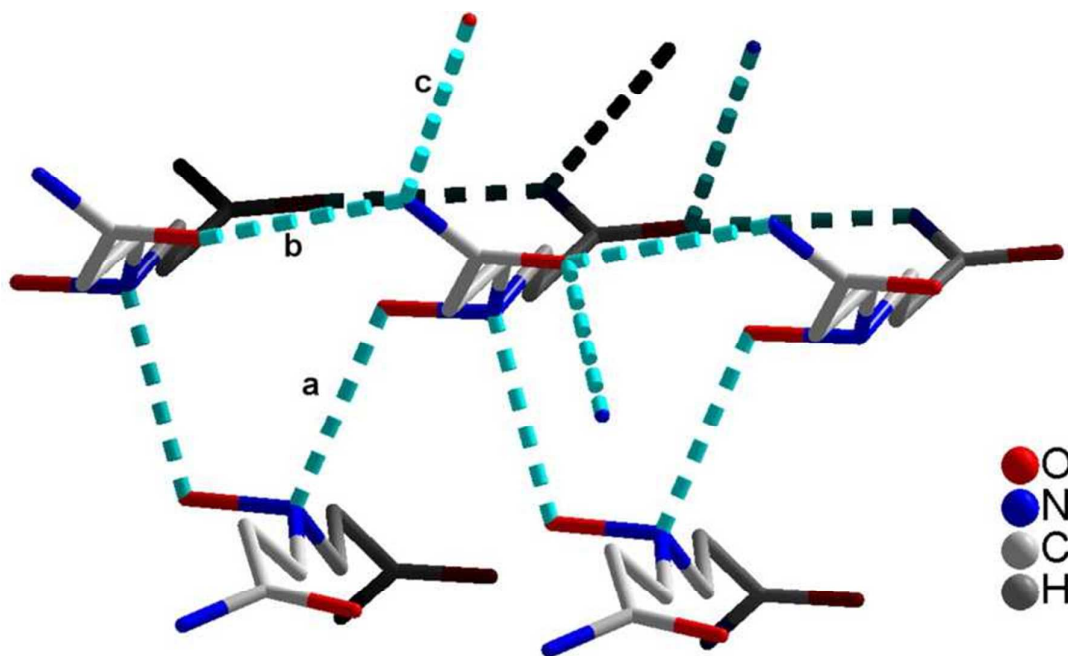
Crystal Structure

Figure S1. Stick diagram Hhydia showing the hydrogen bonding in the crystal lattice. Each molecule is connected with seven other molecules through hydrogen bonds constructing a 3D structure. One molecules is connected with (a) two other molecules through two O(1)-H---N(1) hydrogen bonds {$d_{O(1)-N(1)}$ = 2.846(2) Å}, (b) the two N(2)-H---O(2) and N(3)-H---O(3) bind two more molecules {$d_{O(2)-N(2)}$ = 2.940(3), $d_{O(3)-N(3)}$ = 2.894(3) Å} and (c) the N(2)-H---O(3) and N(3)-H---O(2) {$d_{O(3)-N(2)}$ = 2.976(3), $d_{O(2)-N(3)}$ = 2.979(3) Å} three additional molecules.
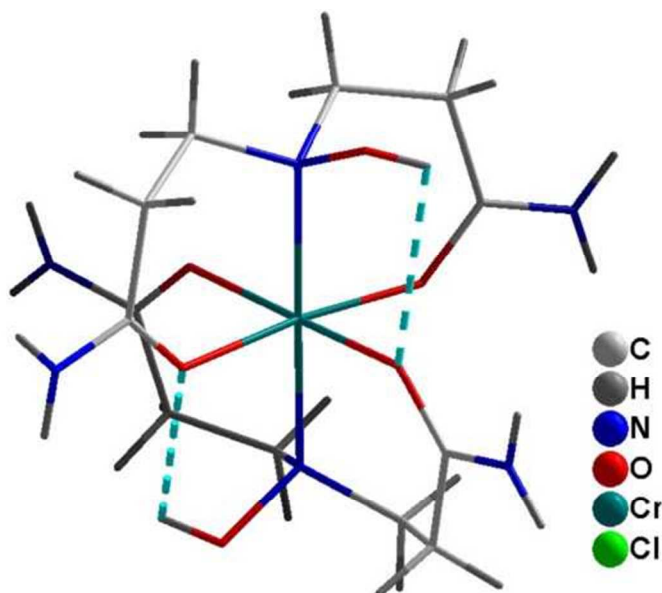
Figure S2. Ball and stick diagram of $[Cr(Hhydia)_2]^{3+}$ showing the intramolecular hydrogenbonding [O(1)-H(1)---O(2), $d_{O(2)-H(1)}$ = 2.583 Å, $\theta_{O(1)-H(1)-O(2)}$ = 97.9(2), $d_{O(2)-O(1)}$ =2.816(4) Å]. The thick brown bonds designate the macrocycle ring that is formed from the two ligands ligation on the metal taking in consideration the two hydrogen bonds.
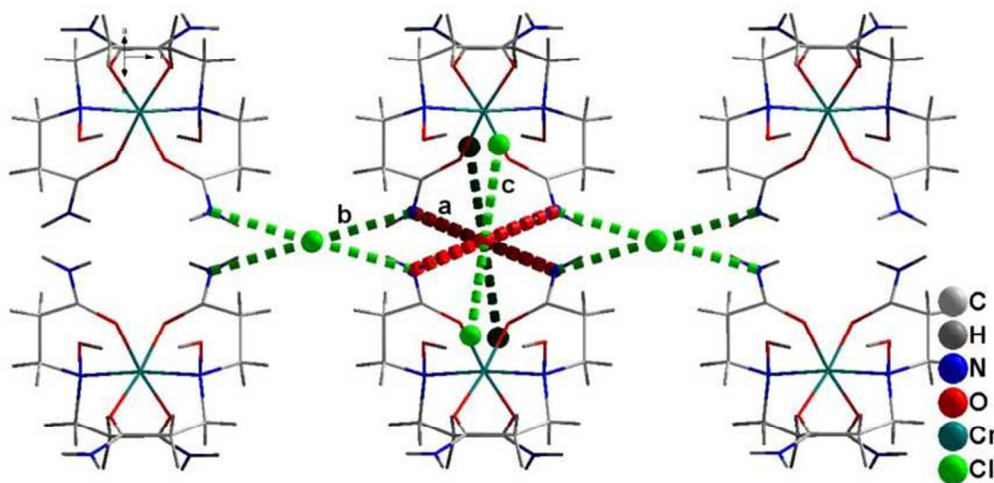
Figure S3. Stick diagram of **1** along *hkl* direction (1, 1, 0) (a) the hydrogen bonds between the N(2)-H_2---O(4) {$d_{N(2)-O(4)}$ = 2.894(4) Å} thick red dashed lines. The N(2) amide nitrogen connect through hydrogen bonds with the free water molecule O(4) to form a dimer. (b) The hydrogen bonds between the N(2)-H_2---Cl(1) {$d_{N(2)-Cl(1)}$ = 3.096(3) Å}. The N(2) connect through hydrogen bonds with Cl(1) anion forming strips of dimers along axic c, thick fragmented green lines along axic c. (c) The free water molecule forms additional hydrogen bonds with Cl(2) {$d_{O(4)-Cl(1)}$ = 3.013(3) Å}, open edge thick green dashed lines. The strips are paralleled to each other and connected though weaker hydrogen bonds (not shown) between the Cl(2) and N(3), {$d_{O(4)-Cl(1)}$ = 3.206(5), 3.234(3)Å}

NMR Spectroscopy
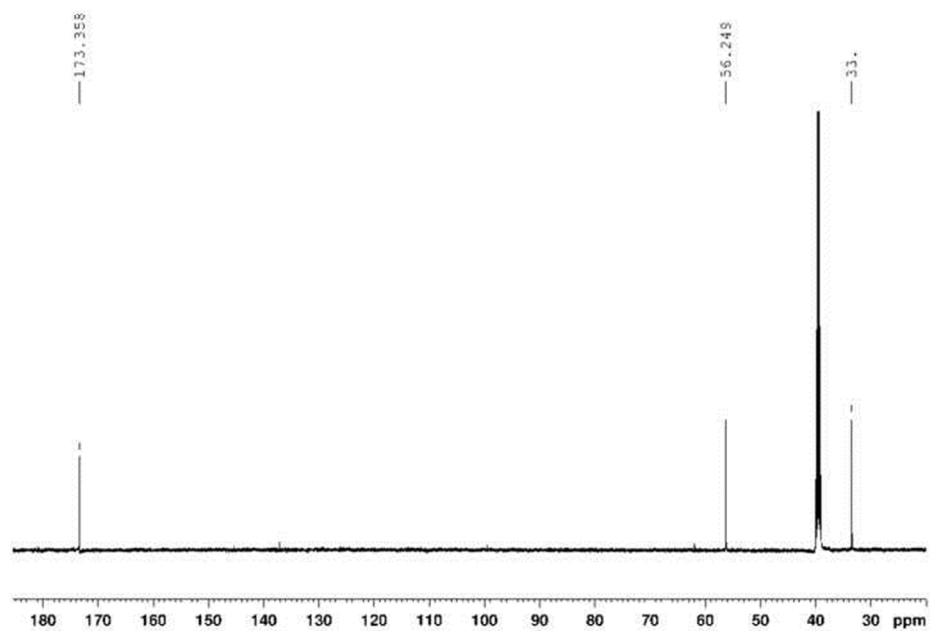
Figure S4. ^{13}C NMR Spectrum of compound Hhydia in DMSO-d$_6$.
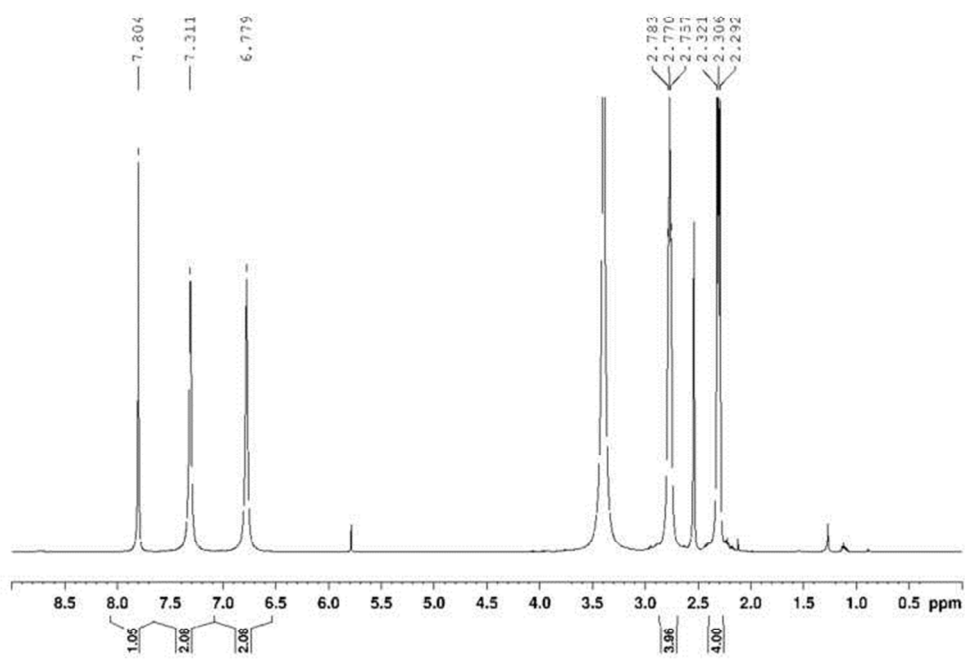
Figure S5. ^{1}H NMR Spectrum of compound Hhydia in DMSO-d$_6$ (500 MHz).
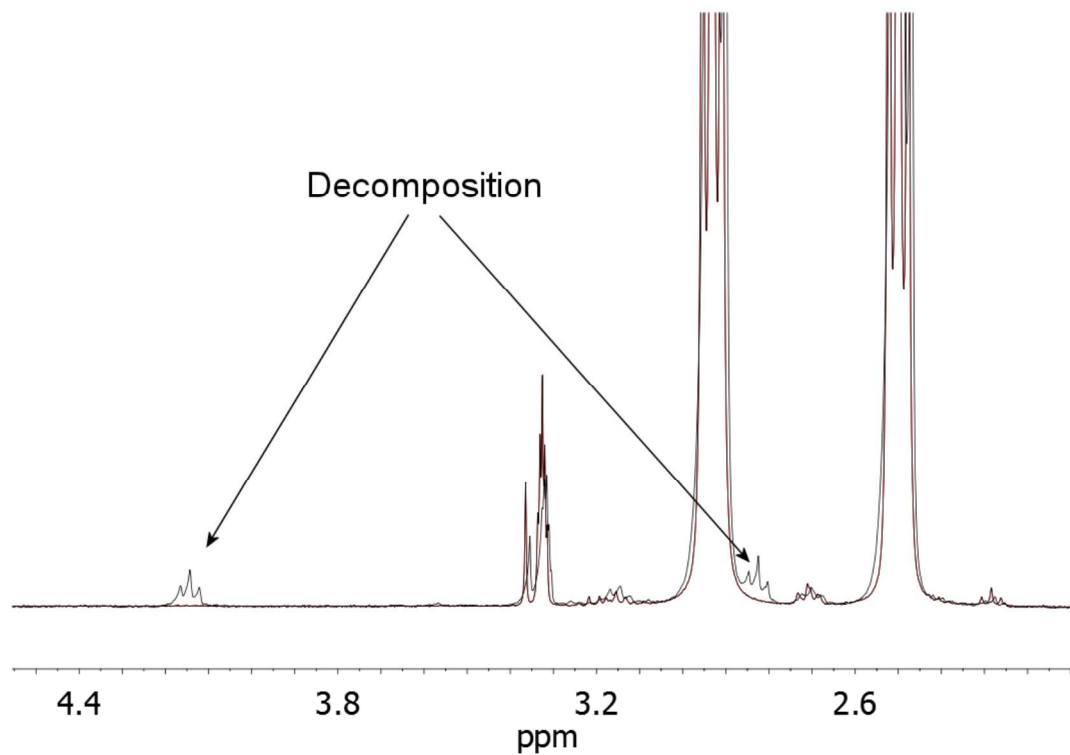
Figure S6. ^{1}H NMR spectra of the ligand Hhydia in CD$_3$OD at time 0 and 12 hours later at 25 ^{o}C. The decomposition peaks are shown with the arrows.
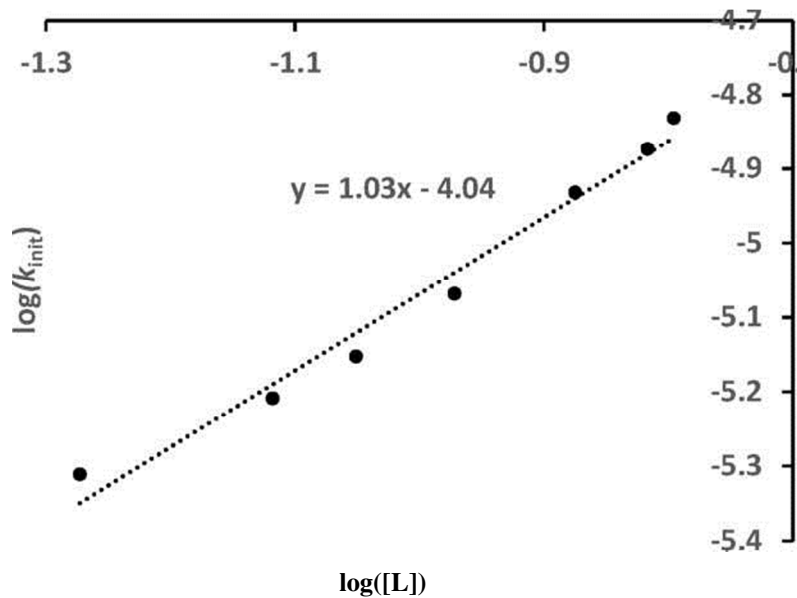
Figure S7. Logarithmic plot of initial rates k_{init}vs[Hhydia] and least square fitting line ($k_{obs298K}$ = 8.7 x 10^{-5} s^{-1} M^{-1}). The formation of the complex was monitored by the absorbance change of the peak at 521 nm.
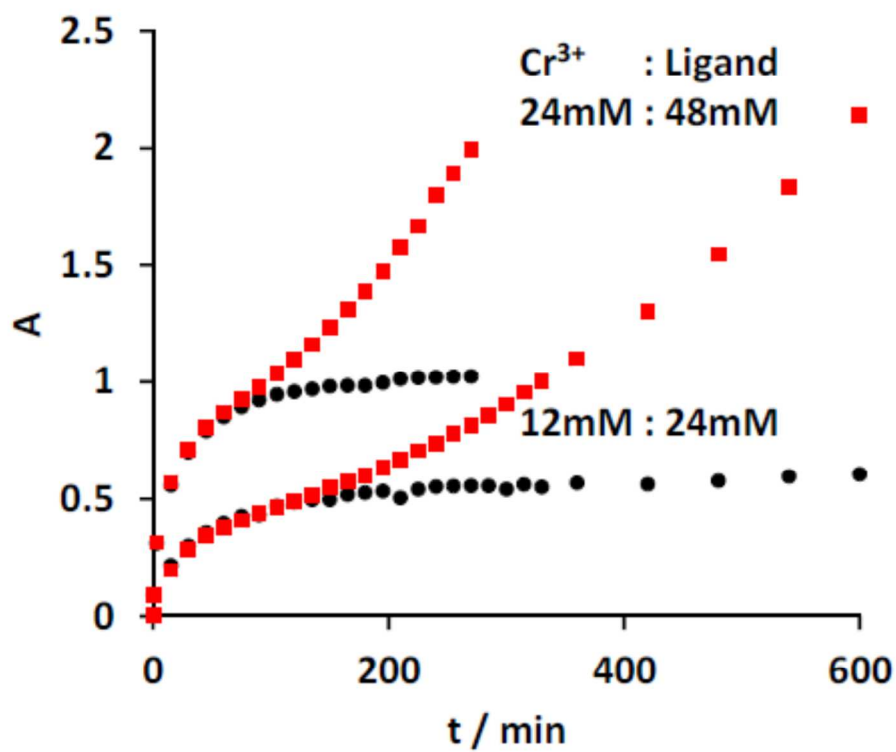
Figure S8. The absorbance (A) at 367 nm (red squares) and at 521 nm (black circles) versus time of two CH$_3$OH solutions containing 24.0 mM Cr(III) , 48.0 mM ligand and 12.0 mM Cr^{3+}, 24.0 mM Ligand.

pH=3.05

ρH=7.18
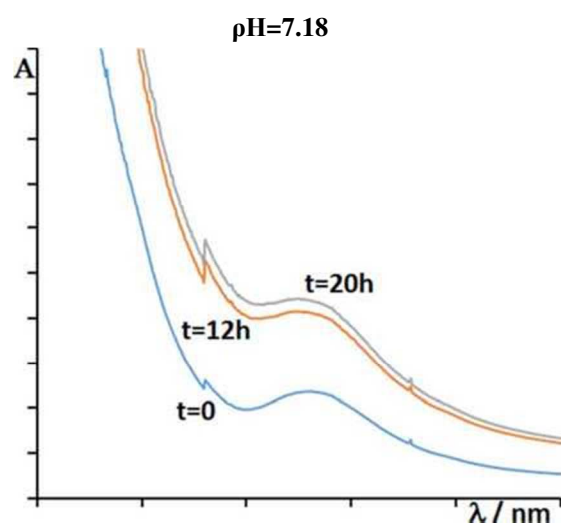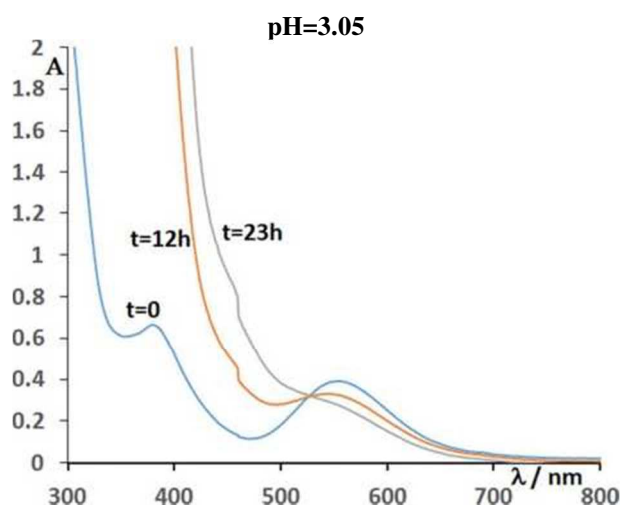
Figure S9. UV-visible spectra of an aqueous solution of **1**·H$_2$O (5.00 mM) at 25 ^{o}C at various times after dissolution of the material. Peaks at pH 3.05, at 556 and 382 nm and at pH =7.18 at 565 nm.

Electrochemistry
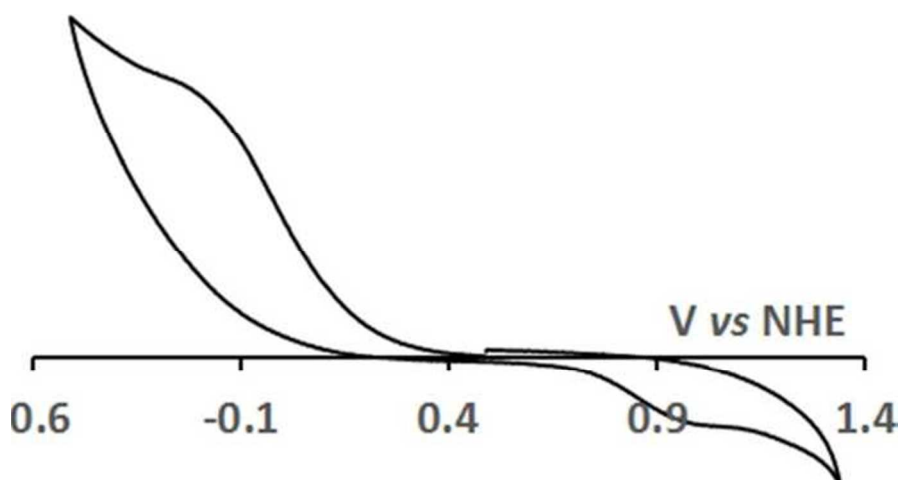
Figure S10. CV of **1**·H_2O in MeOH. The electrochemical measurements were carried out in MeOH extensively purged with N_2 prior to the measurement and 0.1 M tetrabutylammonium tetrafluoroborate was used as supporting electrolyte. All potentials were determined at a scan rate (*v*) of 100 mV s^{-1}. The complex gave the same CV with the free ligand and thus the peaks were assigned as ligand centered, reduction and oxidation of the hydroxylamine moiety.

Optimized geometries by DFT

cis-[Cr^{III}(hydia)Cl$_2$]   *cis*-[Cr^{III}(bipyh)Cl$_2$]
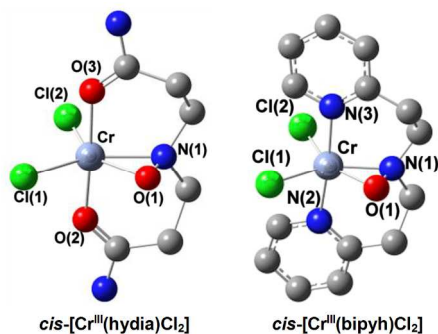
Figure S11. Optimized geometries of the complexes *cis*-[Cr^{III}Cl$_2$(hydia)] and *cis*-[CrCl$_2$(bipyh)] at the B3LYP level (Hydrogen atoms are not shown for clarity).

Crystallographic data

Table S1. Summary of X-Ray Crystallographic and Experimental Data for the compounds $[Cr^{III}(Hhydia)_2]Cl_3 \cdot H_2O$ and Hhydia[a, b]

	$1 \cdot H_2O$	Hhydia
Empirical formula	$C_{12}H_{26}Cl_3CrN_6O_7$	$C_{12}H_2N_6O_6$
Formula weight	524.74	350.39
Crystal system	Tetragonal	Monoclinic
Space group	$P\text{-}4n2$	$I2/a$
Unit cell dimensions		
a (Å)	14.8275(5)	16.035(2)
b (Å)	14.8275(5)	4.8622(5)
c (Å)	10.1100(3)	21.490(2)
$\square$ (deg)	90.0	90.552(9)
Volume (Å^3)	2222.7(1)	1675.4(3)
Z, d (g/cm^3)	4, 1.568	4, 1.389
μ (mm^{-1})	0.920	0.111
$F(000)$	1084	752
θ range	2.80 – 29.31	3.16 – 29.67
Limiting indices	$-20 \leq h \leq 18$ $-20 \leq k \leq 19$ $-13 \leq l \leq 13$	$-21 \leq h \leq 22$ $-5 \leq k \leq 6$ $-29 \leq l \leq 26$
Reflections collected/unique	20298/2863	4954/ 2026
R_{int}	0.0540	0.0317
Data/parameters	2863 / 133	2026 / 129
Goodness-on-fit (GOF) on F^2	1.068	1.152
Final R [$I > 2\sigma(I)$]	$R_1 = 0.0511$ $wR_2 = 0.1300$	$R_1 = 0.0538$ $wR_2 = 0.1710$
R (all data)	$R_1 = 0.0705$ $wR_2 = 0.1433$	$R_1 = 0.0652$ $wR_2 = 0.1799$

[a] Structures were determined at T = 150 and 100 K for $1 \cdot H_2O$ and Hhydia respectively.

[b] Refinement method, full–matrix least–squares on F^2.

Table S2. Interatomic Distances (Å) and Angles (deg) for the Compound Hhydia

Parameter	Value (Å)	Parameter	Value (Å)
O(1)-N(1)	1.451(2)	C(6)-C(5)	1.507(3)
O(2)-C(6)	1.243(2)	N(3)-C(3)	1.326(3)
N(1)-C(4)	1.469(3)	C(4)-C(5)	1.522(3)
N(1)-C(1)	1.471(2)	C(1)-C(2)	1.524(3)
O(3)-C(3)	1.239(2)	C(3)-C(2)	1.512(3)
C(6)-N(2)	1.332(3)		

Parameter	Value (°)	Parameter	Value (°)
O(1)-N(1)-C(4)	105.8(2)	C(6)-C(5)-C(4)	108.9(2)
O(1)-N(1)-C(1)	105.9(1)	N(1)-C(1)-C(2)	113.4(2)
C(4)-N(1)-C(1)	107.8()	O(3)-C(3)-N(3)	122.4(2)
O(2)-C(6)-N(2)	122.4(2)	O(3)-C(3)-C(2)	120.7(2)
O(2)-C(6)-C(5)	120.6(2)	N(3)-C(3)-C(2)	116.9(2)
N(2)-C(6)-C(5)	117.0(2)	C(3)-C(2)-C(1)	109.7(2)
N(1)-C(4)-C(5)	112.8(1)		

Table S3. Interatomic Distances (Å) and Angles (deg) for the Compound $[Cr^{III}(Hhydia)_2]Cl_3 \cdot H_2O$

Parameter	Value (Å)	Parameter	Value (Å)
C(1)-C(2)	1.480(7)	C(6)-N(2)	1.299(6)
C(1)-N(1)	1.486(6)	N(1)-O(1)	1.473(5)
C(2)-C(3)	1.506(6)	N(1)-Cr(1)	2.117(3)
C(3)-O(3)	1.280(5)	O(1)-H(1)	0.8200
C(3)-N(3)	1.296(6)	O(2)-Cr(1)	1.959(3)
C(4)-N(1)	1.467(6)	O(3)-Cr(1)	1.950(3)
C(4)-C(5)	1.509(7)	Cr(1)-O(3)#1	1.950(3)
C(5)-C(6)	1.515(6)	Cr(1)-O(2)#1	1.959(3)
C(6)-O(2)	1.267(5)	Cr(1)-N(1)#1	2.117(3)

Parameter	Value (°)	Parameter	Value (°)
C(2)-C(1)-N(1)	116.1(4)	C(3)-O(3)-Cr(1)	133.4(3)
C(1)-C(2)-C(3)	116.0(4)	O(3)-Cr(1)-O(3)#1	97.2(2)
O(3)-C(3)-N(3)	119.6(4)	O(3)-Cr(1)-O(2)#1	87.7(1)
O(3)-C(3)-C(2)	121.7(4)	O(3)#1-Cr(1)-O(2)#1	173.9(1)
N(3)-C(3)-C(2)	118.7(4)	O(3)-Cr(1)-O(2)	173.9(1)
N(1)-C(4)-C(5)	116.0(4)	O(3)#1-Cr(1)-O(2)	87.7(1)
C(4)-C(5)-C(6)	117.0(4)	O(2)#1-Cr(1)-O(2)	87.8(2)
O(2)-C(6)-N(2)	120.1(4)	O(3)-Cr(1)-N(1)	90.5(1)
O(2)-C(6)-C(5)	123.0(4)	O(3)#1-Cr(1)-N(1)	85.8(1)
N(2)-C(6)-C(5)	117.0(3)	O(2)#1-Cr(1)-N(1)	90.5(1)
C(4)-N(1)-O(1)	103.3(3)	O(2)-Cr(1)-N(1)	93.6(1)
C(4)-N(1)-C(1)	110.6(4)	O(3)-Cr(1)-N(1)#1	85.8(1)
O(1)-N(1)-C(1)	106.5(3)	O(3)#1-Cr(1)-N(1)#1	90.5(1)
C(4)-N(1)-Cr(1)	111.4(3)	O(2)#1-Cr(1)-N(1)#1	93.6(1)
O(1)-N(1)-Cr(1)	114.6(2)	O(2)-Cr(1)-N(1)#1	90.5(1)
C(1)-N(1)-Cr(1)	110.1(3)	N(1)-Cr(1)-N(1)#1	174.3(2)
C(6)-O(2)-Cr(1)	131.0(3)		

NMR Spectroscopic Data

Table S4. NMR Spectroscopic Data (500 MHz, DMSO-d_6) for compound Hhydia

Position	δ_C, type	δ_H (*J* in Hz)	HMBC[a]
3,6	173.3, C		
2,5	33.4, CH	2.31, t	3,1
1,4	56.2, CH$_2$	2.77, t	2,1
A		6.78, s	2,1
a'		7.31, s	1
-O(1)**H**		7.80, s	3

[a]HMBC correlations, optimized for 8.0 Hz, are for protons stated to the indicated carbon

Table S5. SemiquantitativeIntraproton distances determined by NOE for the two molecules in DMSO-d$_6$.

Interproton distances / Å

Proton	2, 5	1, 4
-O(1)**H**	medium	weak
a amide H	medium	weak
a' amide H	weak	weak

Theoretical calculations

Table S6. Selected Calculated Bond Distances (Å) for the Two Conformers of the Ligand, [Hhydia]$_a$ and [Hhydia]$_b$, and its Deprotonated form, [hydia]$^-$, at the B3LYP.[a,b]

	[L^{am}H]a	[L^{am}H]b	[L^{am}]$^-$
N1–O1	1.461(1.452)	1.459	1.439
O1–H1	0.970	0.970	
C1–N1	1.466(1.471)	1.466	1.466
C1–C2	1.527(1.523)	1.527	1.545
C2–C3	1.507(1.509)	1.508	1.507
C3–O3	1.223(1.240)	1.221	1.238
C3–N3	1.348(1.328)	1.371	1.348
N3–H2	1.011	1.011	1.073
N3–H3	1.008	1.009	1.012
H2···O1			1.574

[a]Experimental values for [Hhydia] are given in parentheses for comparison reasons. [b]Numbering scheme as in Figure 10.

Table S7. Selected Calculated Bond Distances (Å) and Angles (deg) for the Species $[Cr(Hhydia)_2]^{3+}{}_a$, $[Cr(Hhydia)_2]^{3+}{}_b$, $[Cr(hydia)_2]^+{}_a$ and $[Cr(hydia)_2]^+{}_b$.[a,b]

	$[Cr(Hhydia)_2]^{3+}{}_a$	$[Cr(Hhydia)_2]^{3+}{}_b$	$[Cr(Hhydia)_2]^+{}_a$	$[Cr(hydia)_2]^+{}_b$		$[Cr(Hhydia)_2]^{3+}{}_a$	$[Cr(Hhydia)_2]^{3+}{}_b$	$[Cr(hydia)_2]^+{}_a$	$[Cr(Hhydia)_2]^{1+}{}_b$
Cr–N1	2.148(2.118)	2.180	2.166	2.053	N1–Cr–O2	91.9(90.4)	91.2	90.1	91.4
Cr–O1	3.006(3.041)	2.936	2.847	1.938	N1–Cr–O3	91.2(85.7)	90.3	88.3	
Cr–O2	1.965(1.950)	1.947	2.048	2.059	N1–Cr–N2	178.7(174.3)	176.7	174.2	116.1
Cr–O3	2.006(1.959)	1.993	2.021	3.325	N1–Cr–O5	87.8(90.5)	92.0	95.8	134.6
Cr–N2	2.148(2.117)	2.180	2.166	2.053	N1–Cr–O6	89.0(85.7)	86.4	85.8	
Cr–O4	3.006(3.039)	2.936	2.847	1.938	O2–Cr–O3	176.9(173.9)	178.1	178.3	
Cr–O5	2.006(1.960)	1.993	2.021	2.059	O2–Cr–N2	89.0(85.8)	86.4	90.1	134.6
Cr–O6	1.965(1.950)	1.947	2.048	3.325	O2–Cr–O5	90.0(87.7)	90.1	90.1	93.1
N1–O1	1.431(1.472)	1.427	1.365	1.393	O2–Cr–O6	90.2(97.2)	88.9	89.3	
N2–O4	1.431(1.472)	1.427	1.365	1.393	O3–Cr–N2	87.8(90.5)	92.0	95.8	
O1–H1	0.981	0.983			O3–Cr–O5	89.9(87.7)	90.9	90.4	
O4–H2	0.981	0.983			O3–Cr–O6	90.0(87.7)	90.9	90.1	
H1···O5	1.851				N2–Cr–O5	91.2(93.6)	90.3	88.3	91.4
H2···O3	1.851				N2–Cr–O6	91.9(90.5)	91.2	90.1	
					O5–Cr–O6	176.9(173.9)	178.1	178.3	
					O1–H1···O5	145.0			
					O4–H2···O3	145.0			

[a] Experimental values for $[Cr(Hhydia)_2]^{3+}$ are given in parentheses for comparison reasons.
[b] Numbering scheme as in Figures 11, and 13.

Table S8. Selected Calculated Bond Distances (Å) and Angles (deg) for the Species *cis*-[Cr(Hhydia)$_2$)Cl$_2$]$^+$ and *trans*-[Cr(Hhydia)$_2$Cl$_2$]$^{+,a}$

	cis-[Cr(Hhydia)$_2$Cl$_2$	*trans*-[Cr(Hhydia)$_2$Cl$_2$		*cis*-[Cr(Hhydia)$_2$Cl$_2$	*trans*-[Cr(Hhydia)$_2$Cl$_2$
Cr–Cl1	2.329	2.386	Cl1–Cr–Cl2	96.5	176.4
Cr–Cl2	2.300	2.340	Cl1–Cr–N1	87.6	90.3
Cr–N1	2.209	2.208	Cl1–Cr–N2	93.3	89.5
Cr–N2	2.218	2.229	Cl1–Cr–O1	176.7	87.6
Cr–O1	2.043	1.955	Cl1–Cr–O2	90.1	90.1
Cr–O2	2.009	1.933	Cl2–Cr–N1	92.6	90.6
H1···Cl1	2.240	2.091	Cl2–Cr–N2	94.8	89.9
H2···O1	1.822		Cl2–Cr–O1	86.6	88.9
H2···Cl2		2.127	Cl2–Cr–O2	173.2	93.4
			N1–Cr–N2	172.3	174.9
			N1–Cr–O1	91.2	90.6
			N1–Cr–O2	86.2	86.7
			N2–Cr–O1	87.5	94.5
			N2–Cr–O2	86.2	88.2
			O1–Cr–O2	86.2	176.4

^{a}Numbering scheme as in Figure 12.

Table S9. Selected Calculated Bond Distances (Å) and Angles (deg) for the Species [Cr(hydia)$_2$Cl$_2$] and [Cr(bipyh)Cl$_2$].[a,b]

	[Cr(hydia)$_2$Cl$_2$]	[Cr(bipyh)Cl$_2$]		[Cr(hydia)$_2$Cl$_2$]	[Cr(bipyh)Cl$_2$]
Cr–Cl1	2.300	2.340(2.346)	N1–Cr–O1	40.7	41.3(42.3)
Cr–Cl2	2.359	2.383(2.338)	N1–Cr–X2	91.05	92.0(91.3)
Cr–N1	2.039	2.022(1.969)	N1–Cr–X3	91.04	92.0(91.4)
Cr–O1	1.964	1.921(1.919)	N1–Cr–Cl1	147.8	146.4(146.2)
Cr–X2[c]	2.026	2.155(2.105)	N1–Cr–Cl2	100.6	106.1(108.4)
Cr–X3	2.026	2.155(2.132)	O1–Cr–X2	92.0	93.6(90.1)
N1–O1	1.393	1.394(1.402)	O1–Cr–X3	92.0	93.6(94.6)
			O1–Cr–Cl1	107.1	105.1(104.1)
			O1–Cr–Cl2	141.2	147.7(150.4)
			X2–Cr–N3	175.7	172.4(175.1)
			X2–Cr–Cl1	90.1	90.1(91.7)
			X2–Cr–Cl2	88.0	86.3(87.1)
			X3–Cr–Cl1	90.1	90.1(88.4)
			X3–Cr–Cl2	87.9	86.4(88.1)
			X2–Cr–X3	11.6	107.5(105.4)

[a]Experimental values for [Cr(bipyh)Cl$_2$] are given in parentheses for comparison reasons.

[b]Numbering Scheme as in Figure S11.

[c]Atom X is O for [Cr(hydia)Cl$_2$] and N for [Cr(bipyh)Cl$_2$].

Calculated and experimental fundamental IR vibrations for Hydia and 1

Table S10. Fundamental IR vibrations calculated and experimental for Hhydia.
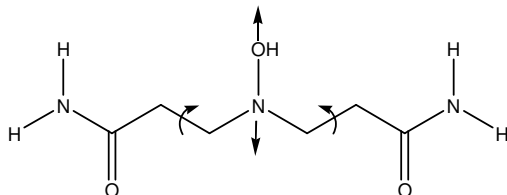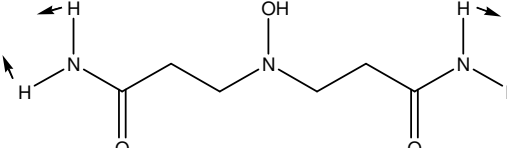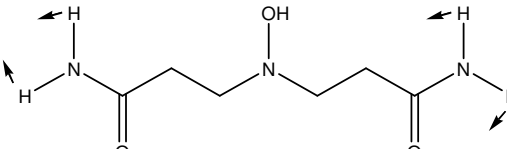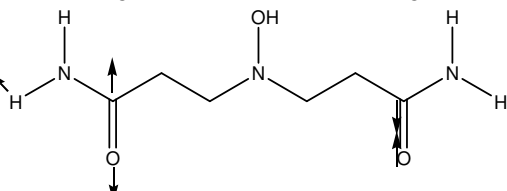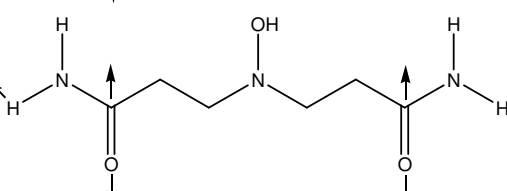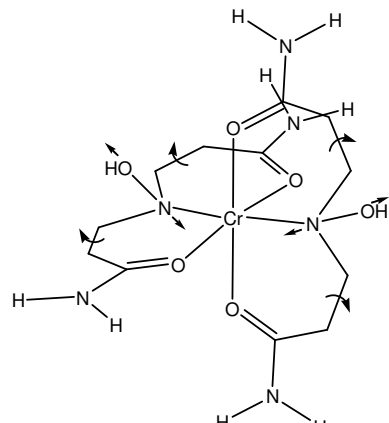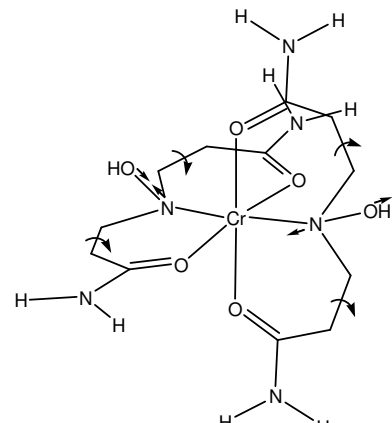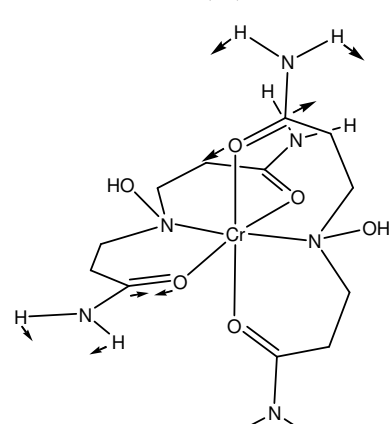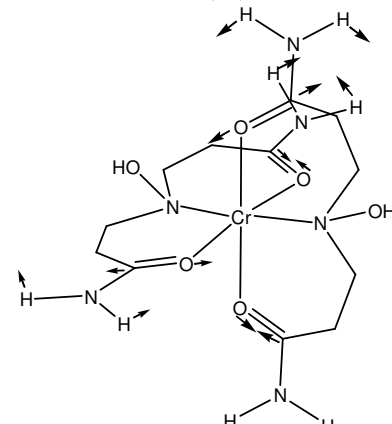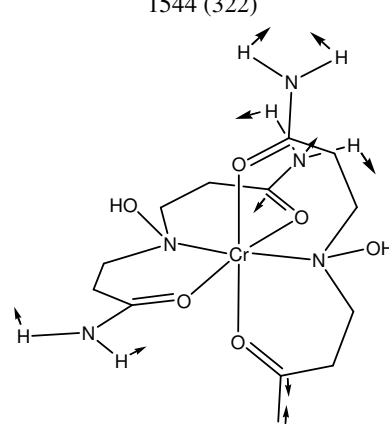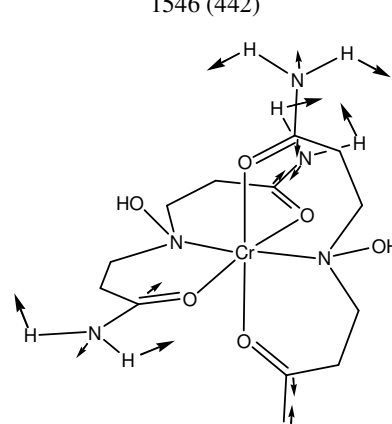

Calc.	Exp.
802 (11)	820m
1580 (203)	1620s
1581 (26)	
1731 (46)	1670vs
1733 (479)	

Table S11. Fundamental IR vibrations calculated and experimental for [Cr(Hhydia)$_2$]$^{3+}$.

Calc.   **Exp.**

895 (24)   896 (28)   834m

1544 (322)   1546 (442)   1547 (343)   1554vs

1645 (234)   1649 (1089)   1650 (869)   1668vs

Experimental Details

NMR Spectroscopy and Sample Preparation. The NMR spectra of 5 mM DMSO-c($_6$ solutions of Hhydia and H$_2$hydia$^+$ Cl$^-$ were recorded in a Bruker AV 500 MHz instrument equipped with a TXI cryoprobe. ^{13}C NMR spectra were typically obtained at sweep-widths of 30 kHz at 125.27 MHz using 32 K data points. The^{1}H-^{13}C HSQC and HMBC experiments were carried out using standard Bruker Topspin 2.1 software, and the parameters were optimized for 145.0 and 8.0 to 2.5 Hz, respectively.2K and 256 transients in the proton and in the carbon dimension, respectively, were collected using 20 repetitions. ^{1}H-^{1}H NOESY experiments were carried out using standard Bruker Topspin 2.1 software, and for 0.1, 0.3 and 0.8 s mixing time and a delay time of 2 s were used. 2 K and 256 transients in the proton dimensions were collected using 8 repetitions.

X-ray Crystallography. Intensity data for the compounds Hhydia and [Cr^{III}(Hhydia)$_2$]Cl$_3$·H$_2$O (1·H$_2$O)were measured on an Oxford Diffraction Gemini A Ultra equipped with an ATLAS CCD detector and aXCalibur III 4-cycle diffractometer [Λ (Mo K_a) = 0.71073 A] radiation at 100 K respectively. In both cases, analytical absorption corrections were applied. The structures were solved by direct methods using the program SHELXS-97[1] and SHELXL-97[1] integrated in the WINGX[2] system and refined on $F2$ by a full-matrix least- squares procedure with anisotropic displacement parameters for all the nonhydrogen atoms based on all data minimizing wR) Σw(|Fo|2 - |Fc|2)/Σw|Fo|2]1/2, R) Σ||Fo| - |Fc||/Σ|Fo|, and GOF) [Σ[w(Fo2- Fc 2)2]/(n - p)]1/2, w) 1/[$σ$2(Fo2) + (aP)2 + bP], where P) (Fo2 + 2Fc2)/3.19. A summary of the relevant crystallographic data and the final refinement details are given in Table S1. The positions of hydrogen atoms were calculated from stereochemical considerations and kept fixed isotropic during refinement or found in a DF map and refined with isotropic thermal parameters. Crystallographic diagrams were drawn using the ORTEP-320 software package at 50% probability level.

EPR Spectroscopy. The cw X-band EPR spectra of the chromium(III) compounds [isolated from ethanol, isopropanol and CH$_3$OH/(C$_2$H$_5$)$_2$O] were measured on an ELEXSYS E500 Bruker spectrometer at resonance frequency ~9.5 GHz and modulation frequency 100 MHz. Powder and frozen methanol solutions of the chromium(III) compounds [isolated from ethanol, isopropanol and CH$_3$OH/(C$_2$H$_5$)$_2$O] were measured at 120 K. The resonance frequency was accurately measured with

solid DPPH (g = 2.0036). The optimization of the spin Hamiltonian parameters and EPR data simulation were performed by using the software package easy spin 4.5.4.[3]

Physical Measurements. IR spectra of the various compounds dispersed in KBr pellets were recorded on a Perkin-Elmer Spectrum GX FT-IR spectrometer. Electronic absorption spectra were measured as solutions in septum-sealed quartz cuvettes on a Jasco V570/UV/Vis/NIR spectrophotometer. Melting points were determined on a Meltemp II apparatus using glass capillaries sealed with vacuum grease, and are uncorrected. HRESI-MS for the ligand Hhydia and its protonated form H_2hydia^+Cl'' were measured in the positive-ion mode with a LTQ-Orbitrap XL (Thermo Scientific, USA) spectrometer. The $H_2hydia+$ Cl^- sample was injected as methyl alcohol solutionand the sample Hhydia as methyl alcohol solutionwith formic acid (0.1%, v/v). Magnetic measurements were carried out on an MK1 MB magnetic susceptibility balance. The magnetic moment was measured by inverse Gouy methodology. The diamagnetic corrections were calculated according to Bain and Berry.[4] Cyclic voltammetry (CV) experiments were conducted on an EG&G Princeton Applied Research 273A potentiostat/galvanostat. Electrochemical procedures were performed with a three-electrode configuration: a platinum disk electrode was used as the working electrode, a platinum wire as the auxiliary electrode and as reference. The potential was calibrated using ferrocene as internal standard (0.63 V vs NHE). All the potential values are referred to NHE. The electrochemical measurements were carried out in MeOH extensively purged with N_2 prior to the measurement and 0.1 M tetrabutylammoniumtetrafluoroborate was used as supporting electrolyte. All potentials were determined at a scan rate (v) of 100 mV s^{-1}.

EIS-MS Experimental and Analyses. All MS data was collected using a Q-trap, time-of-flight MS (MicrOTOF-Q MS) instrument supplied by BrukerDaltonics Ltd. The detector was a time-of-flight, microchannel plate detector and all data was processed using the BrukerDaltonics data analysis 3.4 software, whilst simulated isotope patterns were investigated using Bruker isotope pattern software and molecular weight calculator 6.45. The calibration solution used was Agilent ES tuning mix solution, Recorder No. G2421A, enabling calibration between approximately 100m/z and 3000m/z. This solution was diluted 60:1 with acetonitrile. Samples were introduced into the MS via direct injection at 180μL/h. The ion polarity for all MS scans recorded was negative, at 25 °C, with the voltage of the capillary tip set at 4000V, end plate offset at -500V, funnel 1 RF at 300Vpp and funnel 2 RF at 400Vpp.

Computational Details.The electronic structure and geometries of the chromium complexes and of the ligand studied were computed within the density functional theory using gradient corrected functionals, at the Becke3LYP computational level[5] using the Gaussian-09 package.[6] The effective core potential (ECP) approximation of Hay and Wadt for describing the $(1s^2 2s^2 2p^6)$ core electron for chromium whereas the associated double-ζ quality basis sets were used for the valence shell.[7] The 6-31G(d) basis set used for the remaining atoms.[8] Time-dependent density functional theory (TD-DFT).[9-11] calculations were performed employing the same functional and basis set for the analysis of the excitation energies for both complexes. The geometry optimizations were performed without any symmetry constraint followed by frequency calculations to confirm that a real minimum had been reached. Harmonic vibrational frequencies reported here were determined by the analytical evaluation of second derivatives of the energy with respect to nuclear displacement and were scaled by 0.9614.[12] All energy differences between various conformers or deprotonation energies reported include the zero point correction, whereas in calculating the interaction energy between hydroxylamine ligands and metal fragments, we accounted for both zero point correction and the basis set superposition error (BSSE) by recalculating the monomer energies using the full dimer basis at the optimized geometry of the dimer using the counterpoise method.[13,14]

Comparison of the Stability of *cis*-[Cr^{III}Cl$_2$(hydia)] with *cis*-[Cr^{III}(bipyh)Cl$_2$]

In order to investigate further the potentially unfavorable formation of chromium(III) compound(s) with the deprotonated ligand hydia⁻, a comparative study of the chromium(III) compound, *cis* [Cr^{III}(bipyh)Cl$_2$] (Scheme 5), was carried out. This complex has been prepared and structurally characterized by Ziegler and co-workers,[15] via rection of chromium(III) with the chelating hydroxylamine ligand *N*,*N'*-bis(2-{pyrid-2-ylethyl})hydroxylamine (Hbipyh) (Scheme S1).
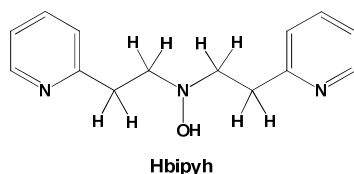
Scheme S1

In the compound *cis*-[Cr[III](bipyh)Cl$_2$] the deprotonated hydroxylamine functionality binds to the chromium atom in a side on mode (Scheme 6, Type I). Thus, the molecular structure of the compound *cis*-[Cr[III](bipyh)Cl$_2$] and of its hydia[-] analogue *cis*-[Cr[III](hydia)Cl$_2$] have been optimized at the B3LYP level. The optimized structures of the complexes are shown in Figure S11, whereas their selected calculated bond lengths and angles are given in Table S7. The two structures are very similar with both ligands binding in a side-on mode, but in *cis*-[Cr[III](hydia)Cl$_2$] the longer Cr–O$_{hydroxylamine}$ bond implies a weaker interaction of the hydroxylamine functionality with the chromium(III). This is also confirmed by the lower adiabatic interaction energy between the [Cr[III]Cl$_2$][+] metal fragment with the deprotonated ligand hydia[-] compared with the deprotonated ligand bipyh[-], being 1351 and 1426 kJ/mol respectively.

Vibrational Spectra of Compounds Hhydia and 1. The calculation of the hessian for the optimized structures of the ligand [Hhydia]$_a$ and of its chromium(III) complex [Cr[III](Hhydia)$_2$]$^{3+}_a$ gave the frequencies of the fundamental vibrations, which are given along with the corresponding experimental normal modes in Tables S8 and S9 respectively. In the spectrum of the ligand the medium band at 820 cm^{-1} (experimental value) is due to the stretching of the N–OH group coupled with torsions of the skeletal carbon atoms. Furthermore, the symmetric and antisymmetric combinations of the bending modes of the two -NH$_2$ groups and of the stretching of the two >C=O groups give strong bands at 1601 cm^{-1} and 1670 cm^{-1} (experimental values). In the spectrum of **1**·2H$_2$O[16] the calculated normal modes are symmetry combinations of modes located in each ligand. The stretching of N–OH group coupled with torsions of the skeletal carbon atoms results in the medium band at 834 cm^{-1} (experimental values). The coordination of the amide oxygen atoms results in a lengthening of the C=O bond and a decrease of the stretching frequency of the >C=O groups (1554 cm^{-1}) (experimental value) in respect to that of the free ligand. This mode is strongly coupled with -NH$_2$ bending. Finally, the bending of the -NH$_2$ groups coupled with C–N stretching gives rise to the very strong band at 1668 cm^{-1} (experimental value).

References

(1) Sheldrick, G.M. *Acta Cryst., Sect. A Found. Cryst.* **2008**, *64*, 112.

(2) Farrugia, L. J. *J. Appl. Cryst.*, **1999**, *32*, 835-838.

(3) Stoll, S.; Schweiger, A. *J. Magn. Reson.* **2006**,*178*, 42.

(4) Bain, G. A.; Berry, J. F. *J. Chem. Educ.* **2008,** *85*, 532-536**.**

(5) (a) Becke, D. *J. Chem. Phys.***1993**, *98*, 5648. (b) Yang, L. W.; Parr, R. G. *Phys. Rev. B* **1988**, *37*, 785.

(6) Gaussian 09, Revision A.02, Frisch, M. J.; Trucks, G. W.; Schlegel, H. B.; Scuseria, G. E.; Robb, M. A.; Cheeseman, J. R.; Scalmani, G.; Barone, V.; Mennucci, B.; Petersson, G. A.; Nakatsuji, H.; Caricato, M.; Li, X.; Hratchian, H. P.; Izmaylov, A. F.; Bloino, J.; Zheng, G.; Sonnenberg, J. L.; Hada, M.; Ehara, M.; Toyota, K.; Fukuda, R.; Hasegawa, J.; Ishida, M.; Nakajima, T.; Honda, Y.; Kitao, O.; Nakai, H.; Vreven, T.; Montgomery, J. A., Jr.; Peralta, J. E.; Ogliaro, F.; Bearpark, M.; Heyd, J. J.; Brothers, E.; Kudin, K. N.; Staroverov, V. N.; Kobayashi, R.; Normand, J.; Raghavachari, K.; Rendell, A.; Burant, J. C.; Iyengar, S. S.; Tomasi, J.; Cossi, M.; Rega, N.; Millam, N. J.; Klene, M.; Knox, J. E.; Cross, J. B.; Bakken, V.; Adamo, C.; Jaramillo, J.; Gomperts, R.; Stratmann, R. E.; Yazyev, O.; Austin, A. J.; Cammi, R.; Pomelli, C.; Ochterski, J. W.; Martin, R. L.; Morokuma, K.; Zakrzewski, V. G.; Voth, G. A.; Salvador, P.; Dannenberg, J. J.; Dapprich, S.; Daniels, A. D.; Farkas, Ö.; Foresman, J. B.; Ortiz, J. V.; Cioslowski, J.; Fox, D. J. Gaussian, Inc., Wallingford CT, 2009.

(7) Hay, P. J.; Wadt, W. R. *J. Chem. Phys.* **1985**, *82*, 299.

(8) Krishnan, R.; Binkley, J. S.; Seeger, R.; Pople, J. A. *J. Chem. Phys.* **1980**, *72*, 650.

(9) Bauernschmitt, R.; Ahlrichs, R. *Chem. Phys. Lett.* **1996**, *256*, 454.

(10) Jamorski, C.; Casida, M. E.; Salahud, D. R. *J. Chem. Phys.* **1996**, *104*, 5134.

(11) van Gisbergen, S. J. A.; Kootstra, F.; Schipper, P. R. T.; Gritsenko, O. V.; Snijders, J. G.; Baerends, E. *J. Phys. Rev. A* **1998**, *57*, 1556.

(12) Scott, A. P.; Radom, L. *J. Phys. Chem.* **1996**, *100*, 16502

(13) (a) Boys, S. F; Bernardi F. *Mol. Phys.* **1970**, *19*, 553. (b) Davidson, E. R.; Chakravorty, S. J. *Chem. Phys. Lett.* **1994**,*217*, 48.

(14) (a) Van Duijneveldt, F. B.; Van Duijneveldt-van de Rijdt, J.G.C.M.; Van Lenthe, J. H.*Chem. Rev.* **1994**, *94*, 1873. (b) Jeziorski, B.; Moszynski, R.; Szalewicz K. *Chem. Rev.* **1994**, 94, *1887*.

(15) Belock, C. W.; Cetin, A.; Barone, N. V.; Ziegler, C. J. *Inorg. Chem.* **2008**, *47*, 7114–7120.

(16) The IR data of the compound **1**·2H$_2$O, prepared in isopropanol, were used since on the basis of the solid state EPR spectra of it, which contains **1** in ≈ 92%.